

Wireless Impedance Measurements and Fault Location on ESRF Vacuum Chamber Assemblies

J. Jacob and G. Gautier: ESRF, BP 220, F-38043 Grenoble Cedex

A.F. Jacob and M. Ikonomou: Inst. f. Hochfrequenztech., Techn. Univ. Braunsch., Postf. 3329, D-W-3300 Braunschweig

F. Caspers: CERN - PS - OP, CH-1211 Genève 23

M. Emmerich: Rosenberger Meßtechnik GmbH Sachsen, Heidestr. 70, D-O-8142 Radeberg

Abstract

The TM wave transmission method and a new fully dispersion compensated TE wave time domain reflectometry (TDR) were applied in order to detect and localize discontinuities on already installed subassemblies of the ESRF vacuum chamber. The use of waveguide modes which require no center conductor allowed in-situ inspection of 13 meter long vessels. The lowest order TM wave has a field distribution close to the TEM like beam induced fields and was coupled via special mode selective antennas in a frequency range between 5 and 18 GHz. The waveguide TDR was performed between 2.7 and 4 GHz, where only the fundamental TE wave propagates: the reflection profile was computed using the time domain facility and dispersion compensation of the network analyzer. With both methods, the obtained responses were similar for all comparable subassemblies and could be interpreted as superposition of the individual responses of the assembled chamber parts. No unexpected response indicating a severe installation error was detected.

1. INTRODUCTION

In the design phase the loss factor of crucial elements of the ESRF vacuum chamber was checked with the wire method combined with the synthetic pulse technique on lab prototypes. For the installation phase new wireless methods were implemented to check the microwave impedance of the vacuum chamber cell by cell during the installation. The cleanliness requirements of UHV forbade the use of a central wire which in any case cannot be accurately positioned in the center of the curved chamber sections. Therefore, waveguide modes were used to detect and localize discontinuities.

2. ESRF VACUUM VESSEL UNDER TEST

Each cell out of the 32 of the storage ring (SR) is equipped with an assembly of 16 pieces of vacuum chambers called CV2 to CV17. The in-situ measurements were performed on all but the 5.35 m long straight CV17 sections dedicated to insertion devices, RF, injection, and diagnostics. For the microwave tests each cell was divided into 2 subsections: one 12.85 m long (CVA) and one 7.45 m long (CVB) as defined below. CV11 was removed to allow the antennas to be mounted. The aim was a comparative measurement of all the CVA and CVB in order to check their correct assembly. The tested elements contain most of the

chamber inhomogeneities that can contribute to the total impedance:

	Length	Main characteristics
CVA:		
CV2:	0.22 m	1 bellow
Valve:	0.10 m	Gate valve with RF shielding
CV3:	3.53 m	2 BPM's + 3 lateral pumping ports
CV4:	0.77 m	2 bellows + 1 bottom pumping port
CV5:	2.83 m	dipole vessel + 2 lateral pumping ports
CV6:	0.32 m	crotch vessel
CV7:	0.39 m	1 bellow
CV8:	2.03 m	2 BPM's + 2 lateral pumping ports
CV9:	0.70 m	1 bellow
CV10:	1.98 m	1 BPM + 2 lateral pumping ports
CV11:	0.71 m	2 bellows + 1 bottom pumping port (removed: no microwave test)
CVB:		
CV12:	2.83 m	dipole vessel + 2 lateral pumping ports
CV13:	0.38 m	crotch vessel
CV14:	0.39 m	1 bellow
CV15:	3.53 m	2 BPM's + 3 lateral pumping ports
Valve:	0.10 m	Gate valve with RF shielding
CV16:	0.22 m	1 bellow

The microwave tests have been performed between november 91 and february 92 on all except cells 3 and 4 at the rate of installation. Windows of typically 3 hours were sufficient for one complete measurement sequence per cell.

3. TM WAVE TRANSMISSION MEASUREMENT

3.1 TM wave method

The TM₁₁ like mode ¹⁾ of the vacuum chamber has fields at the outer boundary which are similar to the TEM like beam induced fields. They differ essentially in the frequency dependence of the phase velocity (waveguide dispersion due to finite TM₁₁ cutoff at 5.2 GHz in the ESRF vessel) and in the field distribution at the center of the aperture. Since the beam impedance is determined by the discontinuities of the walls the TM₁₁ mode has a similar response to local discontinuities as the TEM like beam fields. However, due to the different phase velocity, the TM wave introduces some phase differences when interference between

¹⁾ TM₁₁: lowest order TM wave of a corresponding rectangular waveguide

longitudinally separated points plays a role [1].

The TM11 mode is coupled via special mode selective antennas into a circular waveguide of diameter 47.6 mm designed following [1]: a linearly tapered coaxial line ends abruptly in an annular gap of 3.2 mm radial width. Absorbing material in the hollow center guarantees a smooth transmission over the frequency range up to 18 GHz and rejection of higher order waveguide modes. A 200 mm long tapered transition piece then matches the circular cross section to the actual shape of the ESRF vacuum vessel with a standard ESRF vacuum flange for easy connection to the vessels.

The transmission response S_{21obj} through the portion of vacuum chamber under test is measured with a vector network analyzer (NWA) in a frequency range between 5.2 and 18 GHz. As derived in [1], for a real impedance (e.g. the peak of a resonance or a localized resistive object), the beam impedance Z_B at a frequency f_0 is approximated by

$$Z_B = \frac{Z_0}{2\pi} \sqrt{1 - \frac{f_c^2}{f_0^2}} \left(1 - \left| \frac{S_{21obj}}{S_{21ref}} \right| \right) \quad (1)$$

where $Z_0 = 377 \Omega$ is the free space impedance and f_c the cutoff frequency of the TM wave. An accurate evaluation of eq. 1 assumes that S_{21ref} is the response of comparable but unperturbed reference vessel.

The sensitivity of the method was tested with a 1.1 m long straight vessel having the standard ESRF cross section. A rectangular boring at its center allowed to insert a small test resonator 22.5 mm x 11.25 mm in section and 21.7 mm long, having theoretically a first $\lambda/4$ resonance at 7.5 GHz. The reference response was simply obtained from replacing the resonator by a stub. As expected, an impedance peak of 33 Ω was measured at 7.4 GHz. The test resonator exhibited a rather low quality factor of about 14 which results from the strong loading by the waveguide modes above cutoff.

3.2 Batch TM wave measurements on vacuum vessels

One of the main difficulties was to define a reference measurement for S_{21ref} in eq. 1 since no undisturbed chamber having a length comparable to a CVA or CVB does exist. Therefore, for each vessel, one absolute response was calculated by setting $S_{21ref} = 1$, and one relative response was obtained with S_{21ref} as the response of one common reference cell: CVA/cell 15 and CVB/cell 20 were chosen as showing the most typical responses.

Fig.1 shows as an example the absolute transmission response for the CVA section of cell 18. The lower curve gives S_{21obj} in dB, the upper one the corresponding beam impedance with the normalization $Z/n = Z_B (f_{rev} / f_0)$ where $f_{rev} = 355$ kHz is the revolution frequency of the SR.

The results for S_{21obj} may be summarized as follows:

- ◊ All the measured CVA and CVB showed in principle the same response with only small differences in the height of the dips: no unexpected response indicating a severe installation error was detected. Comparative measurements on single chamber elements revealed that:
- ◊ Dips A in fig. 1 are due to the dipole + crotch vessels.
- ◊ The strong dip B at 8 GHz is created in CV3, 8, 10 and 15 type chambers having lateral pumping ports: this unexpected result of a larger perturbation from lateral than from bottom pumping ports could possibly be explained by a different coupling to modes above cutoff. The wire method did not indicate this behaviour.
- ◊ Dips C in fig. 1: comparable dips were found in the response of shielded bellows. The lab experiment also showed that the bellow response was not very sensitive to incorrect contact of the RF fingers: bad contacts are thus not well detected in the batch measurement.
- ◊ Part D of the response in fig. 1 shows a small depression near 17 GHz, which was proportional to the total length of the vessel and not due to a specific element.

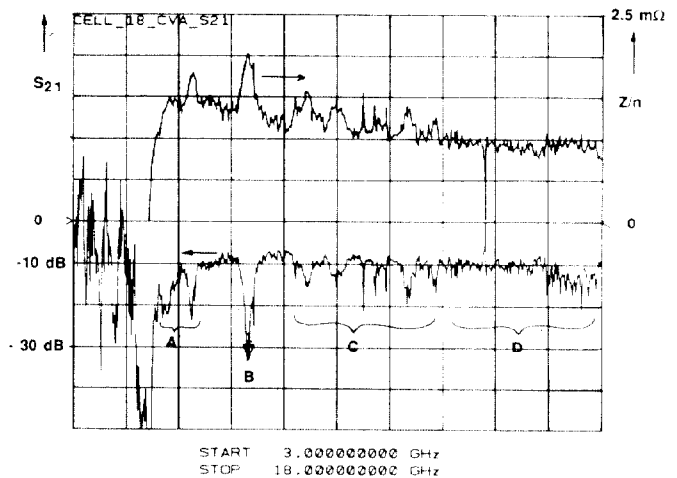


Fig. 1: Absolute S_{21obj} and Z/n for CVA of cell 18

The plot of Z/n in fig. 1 shows the asymptotic behaviour of eq. 1 for small values of S_{21obj} , which leads to relatively small impedance values even for strong transmission dips. Theoretically, modes above cutoff are loading resonant imperfections so as to limit the maximum impedance. But the model leading to eq. 1 assumes a single localized inhomogeneity which is not the situation for the vessels under test here. Therefore, the impedance plots might well be too optimistic and the impedance sum from all the measured cells $Z_{tot}/n < 0.12$ m Ω is probably underestimated.

Relative impedances in the range $Z/n = 0.5$ to 1 m Ω were obtained when using the responses of cells 15 and 20; the spectral distribution adds no extra information to the fact that all the cells have a rather similar response.

4. TE WAVE TDR

4.1 Implementation of TE wave TDR

In order to also localize discontinuities, a fully dispersion compensated waveguide Time Domain Reflectometry was applied for the first time on a vacuum chamber. A TDR is very phase sensitive and a high directivity as well as strong rejection of spurious modes are required. Therefore, the TDR was implemented for the frequency range between 2.7 and 4 GHz, where only the fundamental TE wave propagates (some distance from its cutoff at 2.23 GHz was necessary to limit pulse distortion due to waveguide dispersion). The TE wave no longer simulates the beam fields, and thus the TDR may only be used to localize discontinuities: no quantitative evaluation in terms of beam impedance is possible.

Special antennas have been built in order to launch the TE wave in the vacuum chamber. Having no standard for a matched load, a TRL calibration was necessary for the reflection measurement. The pulse reflectometry was achieved by applying the Fourier transform facility of the HP 8510 NWA on the band limited frequency domain data. In the time domain bandpass mode, the NWA calculates the envelope of the response to a narrow microwave pulse, similar to a radar pulse.

A real microwave pulse would be spread while propagating through a dispersive waveguide, i.e. the time response of the reflection would not give the spacial distribution of the reflectivity. However, the NWA is able to compensate for the waveguide dispersion when computing the Fourier transform. This can be done for one particular location, say z_1 in longitudinal direction, by asking for a corresponding waveguide delay, provided one has also entered the right value for the cutoff frequency (2.23 GHz). Then, the reflection at $t=0$ on the NWA display gives the exact undistorted reflection coming from z_1 , the dispersion compensation being valid only for this particular point. In order to obtain the complete longitudinal distribution of the partial reflections in the ESRF vessels, the reflection at $t=0$ on the NWA display was plotted versus z_1 . Note that for each value of z_1 a complete Fourier transform had to be performed, and it took about 5 minutes to obtain a plot of 200 points resolution.

The method was also checked with the test chamber, and the test resonator as well as an inserted M5 nut could easily be localized with a precision of the order of 1 cm.

4.2 Batch TE wave TDR on vacuum vessels

Fig. 2 shows the longitudinal reflection profile of CVA / cell 18, seen from CV10, together with a scaled sketch of the vessel. It illustrates well the main results obtained:

- ◊ The TE wave dispersion law is altered in the broadened dipole vessel, so that the dispersion compensation is no longer valid beyond CV6. Therefore, all the CVA have been inspected from both ends: CV10 and CV2.
- ◊ The used TE wave is very sensitive to longitudinal slots on

the narrow wall of the vessel: this explains that the higher reflections correspond exactly to the location of the longitudinal RF fingers of the bellow shieldings.

- ◊ A strong reflection also comes from the crotch vessel CV6.
- ◊ A significant response was also obtained from the lateral pumping ports on the narrow walls of the vessels. A higher resolution even clearly shows that the start and the end of these pumping grids launch distinct reflections.
- ◊ As for the TM wave method, no spurious response was detected that would have initiated the reopening of a vessel. The reflection of all the inspected cells show similar results to fig. 2.

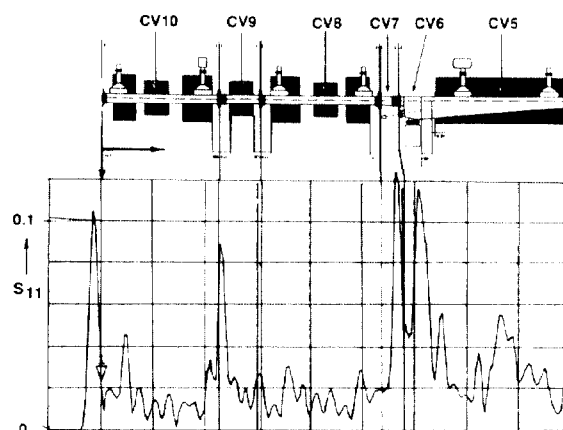


Fig. 2: Dispersion compensated TDR of CVA of cell 18

5. CONCLUSIONS

An almost complete in-situ microwave inspection of the installed ESRF vacuum chambers has been achieved. All comparable chamber sections showed similar intrinsic responses to TM wave transmission and to TE wave TDR. The absence of larger deviations led to the assumption that no severe installation error occurred. The fast achievement of 50 to 100 ms of stored beam seems to confirm this assumption.

The TM wave method is a powerful tool for a wireless inspection. However, further investigations are required in order to obtain a better interpretation in terms of impedance for large chamber assemblies measured outside the lab.

The successful implementation of a fully dispersion compensated TDR using a guided TE mode allowed precise location of discontinuities. Future development should focus on a TM wave TDR in order to be more sensitive to the type of inhomogeneities which contribute to the beam impedance. This will require special attention in order not to create spurious reflections by intermodal coupling.

6. REFERENCES

- [1] G.R. Lambertson, A.F. Jacob, R. A. Rimmer and F. Voelker "Techniques for Beam Impedance Measurements Above Cutoff", in EPAC'90 Proceedings, Nice, June 1990, pp. 1049-1051.